

## INFLUENCE OF ANNEALING HEAT TREATMENT ON PITTING CORROSION RESISTANCE OF STAINLESS STEEL TYPE 316L

Amirreza Bakhtiari<sup>1\*</sup>, I. Berenjani<sup>2</sup>

<sup>1</sup>Technical inspection section, Yadak Sazan Pakhsh Omid (YSPO), Tehran, Iran

<sup>2</sup>Technical inspection & corrosion engineering, National Iranian south  
oilfield company (NISOC), Ahvaz, Iran

Received 14.03.2014

Accepted 10.04.2014

### Abstract

The effect of annealing heat treatment on pitting resistance of stainless steel type 316L has been studied using Tafel polarization and ASTM G150 for estimating of the pitting potential and CPT, respectively. The materials were tested in 3.5% NaCl solution. The chemical composition of the material was analyzed via optical emission spectrometry. It was found that the sample treated at 940°C shows better pitting corrosion resistance than samples treated at 520°C and 820°C. The treatment at 940°C produced two types of morphologies, austenitic-ferritic matrix with  $\delta$ -ferrite and only small amount of the  $\sigma$  phase. In the range up to 820°C the  $\sigma$  phase embedded in the  $\gamma$  phase matrix and at  $\delta/\gamma$  interface was causing brittleness of the material and aggravated corrosion resistance. The treatment at 940°C produced the microstructure which prevented the corrosion attack to develop. It was revealed that the pitting size in samples treated at 520°C and 820°C is greater than that at 940°C. In addition, depth of pitting has been considered as a factor of pitting corrosion resistance. The depth of pitting in sample treated at 940°C is low since the pitting is almost superficial, while the pitting size in samples treated in 520°C and 820°C is higher and deeper.

*Keywords: stainless steel 316L, annealing heat treatment,  $\sigma$ -phase, Tafel polarization, pitting resistance, CPT*

### Introduction

Type 316L stainless steel is not only characterized by high strength at elevated temperatures, but is also recognized for a wide applications requiring corrosion resistance superior to Type 304. Typical uses include exhaust manifolds, furnace parts, heat exchangers jet engine parts, pharmaceutical and photographic equipment, valve and pump, chemical equipment, digesters, tanks, evaporators, pulp, paper and textile processing equipment, parts exposed to marine atmospheres and tubing. Type 316L is

---

\*Corresponding author: A. Bakhtiari: bakhtiari.amirreza@gmail.com

used extensively for weldments where its immunity to carbide precipitation due to welding assures optimum corrosion resistance [1]. Austenitic AISI 316L is considered to be one of the most resistant of common stainless steels under marine environments, and due to its good mechanical properties at elevated temperatures, and easy fabricability, is an important structural material for many industrial unit especially the desalination plants. The most common cause of failure of 316L stainless steel in marine environment is pitting and crevice corrosion, which are very dangerous, since the material can quickly be penetrated despite the fact that its general corrosion rate is very low [2].

Pitting corrosion is one of the most destructive and insidious forms of corrosion because of the localized nature of the attack and the difficulty associated with the prediction of pitting tendency. Many investigations have been performed to understand the pitting corrosion phenomenon. Recently, major efforts have been directed toward the characterization of pitting corrosion by the determination of two characteristics of pitting, namely, pitting potential, and protection potential. In general, the pitting potential ( $E_p$ ) is the potential above which passive alloys are susceptible to pitting corrosion in halide solutions, but below which pits cannot be formed, although existing pits can grow if the potential is higher than protection potential. The protection potential ( $E_{pp}$ ) is the potential value such that at potential higher or equal to this potential, pit can propagate, but if the potential is below, metal remains passive. To obtain the precise data, the pitting potential can be determined only by recording the current density vs. time relationship at various constant potential using a new sample for each curve. For precise protection potential determination recording of the current density vs. time curve at constant potential should be preceded by activation of the sample at high anodic potential corresponding to easy pit nucleation. Measurements of changes in anodic potential at constant current density starting from the corrosion potential and measurement of potential drop vs. time at high constant current density can be used. Potentiodynamic pitting test is the common technique for rapid evaluation of the relative pitting tendencies of a series of alloys. Both pitting potential and protection potential are the important parameters from the theoretical point of view. For practical purpose, protection potential is more useful because it indicates the range of potentials more negative than protection potential within which pitting will not occur. Pitting potential depends on the composition of the bulk solution, and on the surface condition of metal, while protection potential depends upon the composition of the solution contained in pits [2-6].

In this investigation, the role of annealing heat treatment on pitting corrosion behaviour of stainless steel type 316L was evaluated and validated.

### **Experimental procedure**

Commercially produced type 316L stainless steel sheet material of 3 mm thickness was used during tests. The composition of the material is given in Table 1. All the tests were carried out three times and the average of results was considered as the final report.

Table 1 Chemical composition of stainless steel 316L (wt.%)

C	Si	Mn	P	S	Cr	Ni	Mo
0.04	1.00	2.00	0.045	0.030	0.058	10.00-14.00	2.00-3.00

The samples have prepared in 20mm × 40mm × 5mm dimension. The samples were polished using carbide papers from 80 to 1200 grit. Finally, samples washed with ethanol and pure water and were polishing with 0.3 μm of Al<sub>2</sub>O<sub>3</sub> powder. The electrochemical etch has done in 0.6 HNO<sub>3</sub> in 1.1 V potential for 2 minutes.

Scanning electron microscopy (SEM) was employed to study the effect of annealing heat treatment on microstructure and phase transformation. In addition, pit morphology studied using SEM.

The electrochemical technique was used to obtain pitting potential, protection potential, and corrosion rate for AISI 316L under various conditions, using EG&G model 273 potentiostat/galvanostat with model 342 soft corrosion software. A saturated calomel electrode was used as the reference electrode. Graphite electrodes were used as counter

The critical pitting temperature (CPT) was obtained in two ways, either by performing a series polarization tests at a fixed temperature or by using ASTM G150. The diagram used for CPT is illustrated in Fig 1.

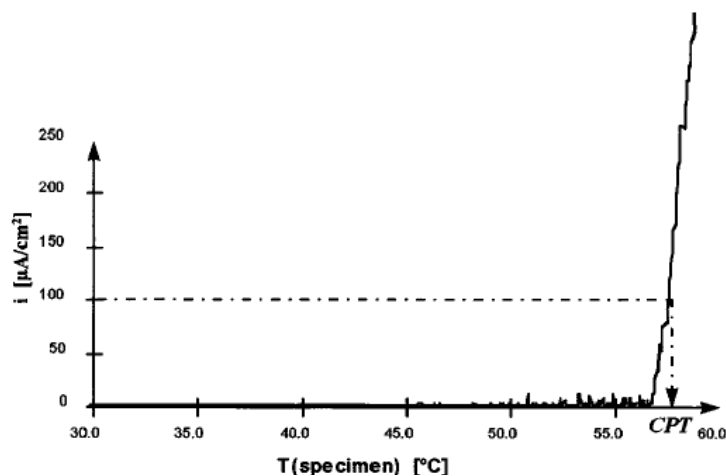


Fig 1. Determination of CPT.

The chemical composition of the material was analyzed via optical emission spectrometry.

Based on the chemical composition, the values of  $Cr_{eq}$  and  $Ni_{eq}$  were calculated according to the following expressions:

$$Cr_{eq} = (\%)Cr + [(1.5). (\%)Si] + [(1.4). (\%)Mo] + (\%)Nb - 4.99$$

$$Ni_{eq} = (\%)Ni + [(30). (\%)C] + [(0.5). (\%)Mn] + [26(\%)N - 0.02] + 2.77$$

The solution annealing heat treatment recommended for this material was performed in an electric furnace with a heating capacity of 1300°C. The solution

annealing heat treatment at 940°C for 2h was carried out to completely dissolve all the precipitates in the austenitic matrix, forming an unsaturated solid solution. After this solution annealing heat treatment, followed by water quenching, the samples were aged at various temperatures ranging from 520–940°C for 2h.

## Results and discussion

### *Microstructure studies*

The sample annealed at 520°C, displays a microstructure composed of only two phases: the austenite matrix consisted of  $\sigma$ -phase and the  $\delta$ -ferrite precipitated in the form of islands, as illustrated in Fig. 2.

The  $\sigma$ -phase is a nonmagnetic inter-metallic phase composed mainly of iron and chromium (Fe-Cr), which forms in ferritic and austenitic stainless steels during exposure at the temperature range 520°C to 950°C, causing loss of ductility and toughness. Cracking may also occur if the component was impact-loaded or excessively stressed during shutdown or maintenance work. The presence of considerable amounts of  $\sigma$ -phase is unacceptable due to its detrimental influence on corrosion and mechanical properties. However, small amounts of  $\sigma$ -phase that formed at certain temperature intervals might be without significance in some applications.

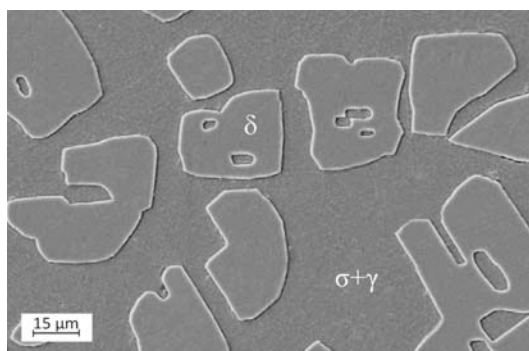


Fig 2. SEM micrograph of the sample treated at 520°C for 2h.

In addition, the  $\sigma$ -phase is a brittle, intermetallic phase with high hardness. They arise, when a cubic body-centered and a cubic body-centered metal coincide, whose atomic radius correspond with a low deviation (8%) [7-8]. The  $\sigma$ -phase forms predominantly out of  $\delta$ -ferrite, because in high alloyed chromium-nickel-steel the composition of the  $\delta$ -ferrite is similar, whereas intermetallic phases precipitated at the  $\delta/\gamma$  interfaces or at the ferrite grain boundaries lead to aggravated corrosion resistance [4]. Ferrite structure has a form of body centered cubic (bcc); this structure has enough space for penetrated interstitial atoms. Furthermore, increasing the space between atoms in bcc structure augments internal energy, and thus decreases corrosion resistance. The carbon atoms cannot be dissolved in ferritic matrix more than 0.025% at 720°C. When the temperature is decreased the amount of dissolved carbon in the ferritic matrix is also decreased [9-10].

It is clear from Fig 3, that a developed pit with the deep depth was formed. Excessive pits could debilitate corrosion performance of stainless steel. It's assumed the

composition of austenite matrix with  $\sigma$ -phase even in small amount of  $\sigma$ -phase could decrease pitting corrosion resistance [7].

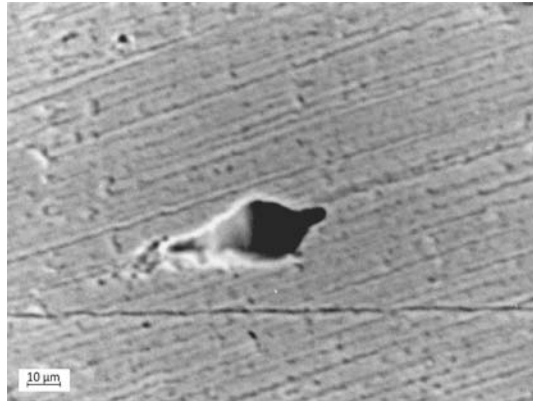


Fig 3. SEM micrograph of pit in specimen treated at 520°C.

The microstructure of the sample annealed at 820°C for 2h is shown in Fig. 4. As a result of transformation  $\delta \rightarrow \gamma + \sigma$  island of the  $\gamma$  phase were formed mixed with ferrite and the  $\sigma$  phase which morphology is in the form of thin lamellae that pointed with arrows in Fig. 4. However, the  $\sigma$ -phase may appear as small rounded particles formed at the  $\sigma/\gamma$  interface (see arrow in Fig. 4). It is not quite clear whether small intragranular particles are  $\sigma$ -phase or  $M_{23}C_6$  carbides. It should be noted, that the ferrite is difficult to identify because at that temperature, its volumetric concentration is very low, i.e. about 3.0 %. However,  $\sigma$ -phase has a grave effect on corrosion resistance, its estimate that the composition of  $\sigma$ -phase and  $\delta$ -ferrite could decrease harmful effect of  $\sigma$ -phase and improve corrosion resistance [11].

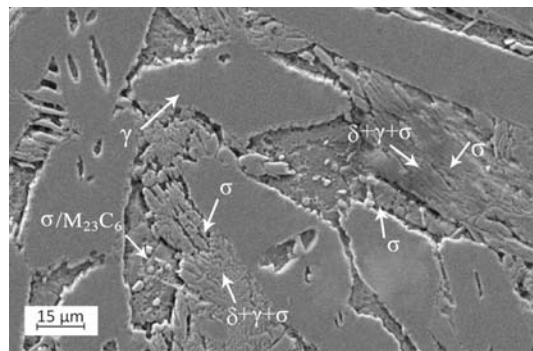


Fig 4. SEM micrograph of the sample treated at 820°C for 2h.

The characteristics of pit in fig 5, has revealed a number of pits. The depth of pits is lesser than depth of pits that has formed at 520°C.

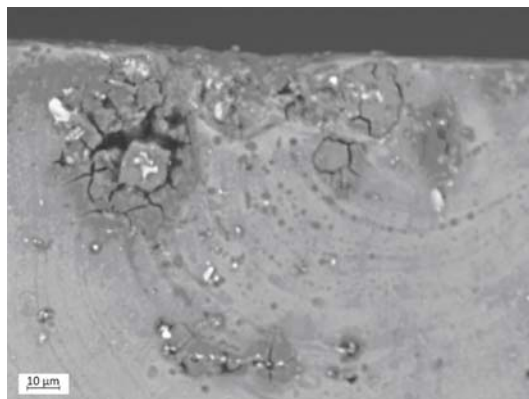


Fig 5. SEM micrograph of pits in specimen treated at 820°C.

The treatment at 940°C (Fig. 6) produced different microconstituents, i.e. islands consisting of the mixture of  $\gamma$ ,  $\delta$ -ferrite and  $\sigma$ -phases, surrounded by the matrix of the  $\gamma$  phase. The  $\delta$  phase appears in the form of elongated thin rods in the  $\gamma$  phase matrix. Significant appearance of the  $\sigma$  phase was recorded at temperatures higher than 520°C, but at 940°C the amount of this phase was significantly decreased. At temperatures above 1000°C the  $\sigma$  phase may be completely dissolved. The dissolving of  $\sigma$ -phase above starts above 900°C, by increasing temperature dissolving rate increased and  $\sigma$ -phase will completely disappeared in high temperature. Disappearing of  $\sigma$ -phase and decreasing amount of  $\sigma$ -phase could enhance corrosion resistance [9-10].

The  $\sigma$ -phase is not only undesirable because of its embrittled effect, but also because of its characteristic, to withdraw chromium out of the matrix. The consequence of this is a drastic deterioration of the stability against corrosion. When sigma-phase precipitates out of the delta-ferrite, also austenite is formed through chromium and molybdenum decrease [8]. The characteristic of the  $\sigma$ -phase shows very brittle, bad impact strength and very low corrosion resistance [7].

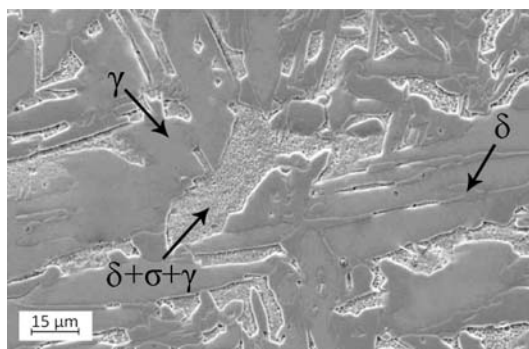


Fig 6. SEM micrograph of the sample treated at 940°C for 2h.

SEM investigation has shown the superficial pits on the surface (Fig. 7). These scattered pits with have no important destructive effect on corrosion behaviour of stainless steel 316L.

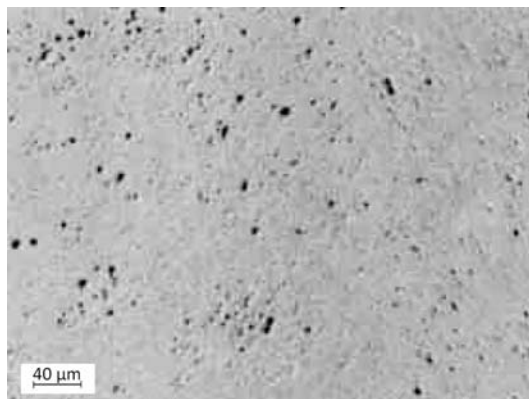


Fig 7. SEM micrograph of pits in specimen treated at 940°C.

#### Analysis of corrosion behaviour

The ASTM G150 method is perhaps the only standardized electrochemical method that allows comparison of pitting data between testing laboratories. Consequently, it was decided to include this relatively new method in the study [2].

The cycling polarization experiments have involved testing at several combinations of chloride concentration and temperature. Besides determining the dependence of the critical pitting potential, the tested levels were selected to obtain the CPT as precisely as possible. The CPT test matrix and obtained pitting potential are listed in Tables 2 and 3.

Table 2 Critical pitting temperature determined using ASTM G150

Specimens	PRE <sup>a</sup>	CPT, °C
Treated in 520 °C	27	16.7
Treated in 820 °C	29.5	18.1
Treated in 940 °C	37	57.4

a. Pitting resistance equivalent, PRE: Cr+3.3 Mo+16 N.

Table 3 Comparison of obtained critical pitting temperature (CPT, °C) using polarization Tafel and ASTM G150 tests

Specimens	Polarization Cl <sup>-</sup> , mg/l	ASTM G150 Cl <sup>-</sup> , mg/l
Treated in 520 °C	9	14±2
Treated in 820 °C	14	16±2
Treated in 940 °C	45	55±3

As it can be seen from Tables 1 and 2, PRE as a factor of pitting resistance increased at the heat treatment temperatures 520°C, 820°C and 940°C, respectively. As above mentioned, the phase transformation was the main cause for these alterations. The sample treated at 940°C, shows superior PRE. Electrochemical techniques and cyclic potentiodynamic results indicate that this sample is high resistant to pitting corrosion due to its repassivation properties are reduced as temperature increases. It's clear, the

surface can be chemically passivated to enhance corrosion resistance; passivation reduces the anodic reaction involved in the corrosion process. In spite of this fact sample treated at 940°C has shown better pitting resistance because of austenite structure [4]. Comparison between the results obtained in 3.5% NaCl solution suggested a decrease in the pitting resistance at high temperatures [5].

With increasing temperature in both solutions the passive film was found to become more porous, and hence less protective. However, at temperatures above 800°C, the loss of film protectiveness is more pronounced in chloride solutions, in which pitting occurs. Pitting morphology was found to be strongly temperature dependent: isolated and deep pits were found up to 800°C, whereas at higher temperatures a broad, shallow and more benign type of attack was detected. It was concluded that the changes in the pitting behaviour of 316L at temperatures below and above 800°C are associated to a temperature-affected variation of the protective properties of the passive film [5-6]. Increasing annealing temperature from 520°C to 940°C elevates the critical pitting temperature, whereas with further increase the annealing temperature above 900°C enhance the critical pitting temperature. The samples annealed at 940°C for 2h exhibit the best pitting corrosion resistance with the highest critical pitting temperature. The pit morphologies show that the pit initiation sites transfer from austenite phase to ferrite phase as the annealing temperature increases. The aforementioned results can be explained by the variation of pitting resistance equivalent of volume fraction of ferrite and austenite as the annealing temperature changes [10-13]

### Conclusion

Phase transformation has a great effect on the corrosion behaviour of stainless steel 316L. The  $\sigma$ -phase begins to precipitate at annealing temperatures starting from 520°C and being completely dissolved in the matrix above 940°C. At heat treatment of 520°C, because of austenite matrix composited with  $\sigma$ -phase made matrix brittle and prone to pitting corrosion, also  $\delta$ -ferrite precipitated in islands that has brittle structure, pits have deep depth. The composition of austenite matrix with  $\sigma$ -phase even in small amount of  $\sigma$ -phase could decrease pitting corrosion resistance. The sample that treated at 820°C, have austenite matrix composited with  $\sigma$ -phase and  $\delta$ -ferrite. The composition of  $\sigma$ -phase and  $\delta$ -ferrite could decrease harmful effect of  $\sigma$ -phase and improve corrosion resistance. At the range of 520-820°C the chromium carbides distributed in austenite matrix consisted of  $\sigma$ -phase and  $\delta$ -ferrite. Because the  $\sigma$ -phase goes in dissolving at temperatures above 900°C, sample treated at 940°C indicated better corrosion behaviour. Despite this fact, increasing temperature decreased pitting resistance, specimen treated at 940°C shows better pitting resistance at high temperature because of austenitic-ferritic matrix with  $\delta$ -ferrite and small amount of  $\sigma$ -phase.

### Acknowledgements

The authors would like to thank Isfahan refinery laboratories staff and R&D unit engineers for helping with the samples. Assistance received from SEM and chemistry laboratories staff of Materials Engineering Department of Isfahan University of Technology (IUT) is also appreciated.



**References**

- [1] Y. Maehara, Y. Ohmori, J. Murayama, N. Fujino, T. Kunitake, *Met. Sci* 17 (1983) 541–547.
- [2] Alonso, N. Análise do método potenciodinâmico de determinação do potencial de pite. Doctoral Thesis (Materials Science and Engineering) — scola Politécnica da Universidade de São Paulo — USP — São Paulo, 1992.
- [3] SB. Kim, KW. Paik, YG. Kim, *Mater. Sci. Eng A247* (1998) 67–74.
- [4] R. Guo, and M.B. Ives, *Corrosion*, 46,125,1990, NACE
- [5] E. Blasco-Tamarit, A. Igual-Muñoz, J. García Antón, D. García-García, *Corros. Sci* 50 (2008) 1848–1857.
- [6] R.M. Carranza, M.G. Alvarez, *Corros. Sci* 38 (1996) 909–925.
- [7] S. Niknafs, In-situ studies of delta-ferrite/austenite phase transformation in low carbon steels, Master of engineering by research Thesis, University of Wollongon, Australia (2007).
- [8] I. Berenjani, Investigation of corrosion behavior of austenitic welded stainless steel, M.Sc Thesis, Isfahan University of Technology, Iran (2009).
- [9] R.E. Reed-Hill, *Physical metallurgy principles*, second ed., D. Vannostrand company, New York, 1991.
- [10] D.A. Porter, K.E. Easterling, *Phase transformation in metals and alloys*, second ed., Chapman & Hall, New York, 1992.
- [11] T. Mathiesen, J. V. Hansen, In: *Duplex World 2010 Conference: Beaune, France, October 2010*.
- [12] Hua Tan, Yiming Jiang, Bo Deng, Tao Sun, Jin Li, *Mater. Charact* 60 (2009) 1049–1054.
- [13] Z. Szklarska-Smialowska, *Corros. Sci* 44 (2002) 1143–1149.